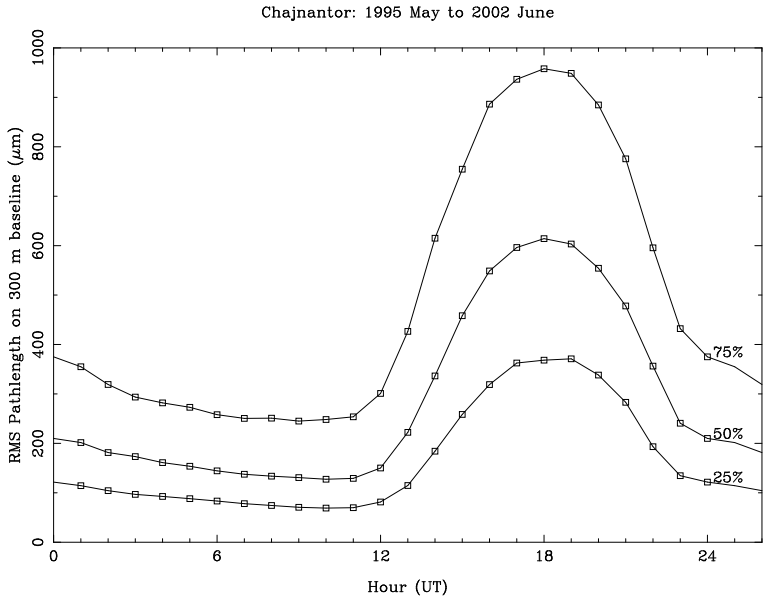

Fig. 5.— Diurnal variation of quartiles of measured phase fluctuations at Chajnantor referred to the zenith.

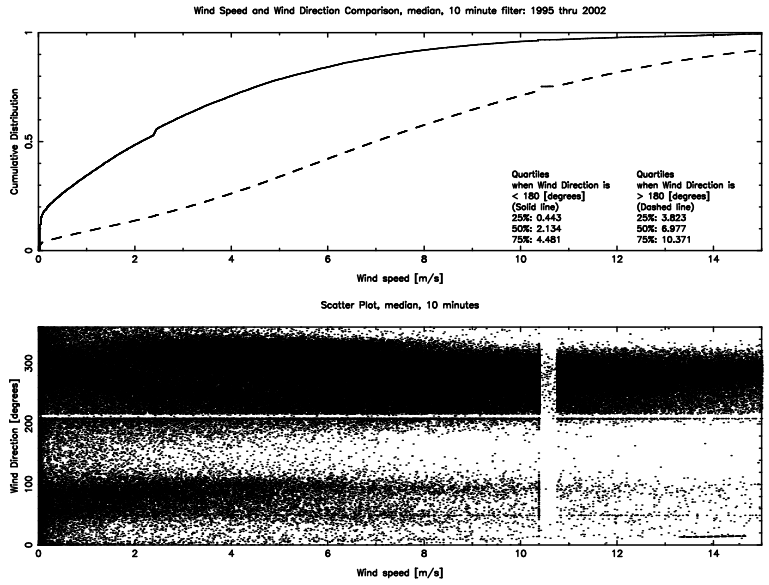

Fig. 6.— Cumulative distributions of westerly and easterly wind speeds measured at Chajnantor.

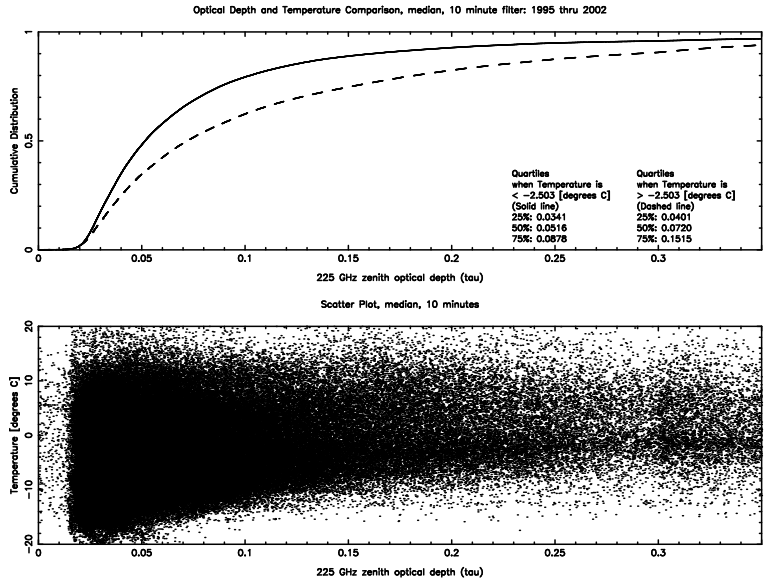

Fig. 7.— Cumulative distributions of the 225 GHz zenith optical depths (τ_{225}) measured at Chajnantor when the temperature was above or below the median.

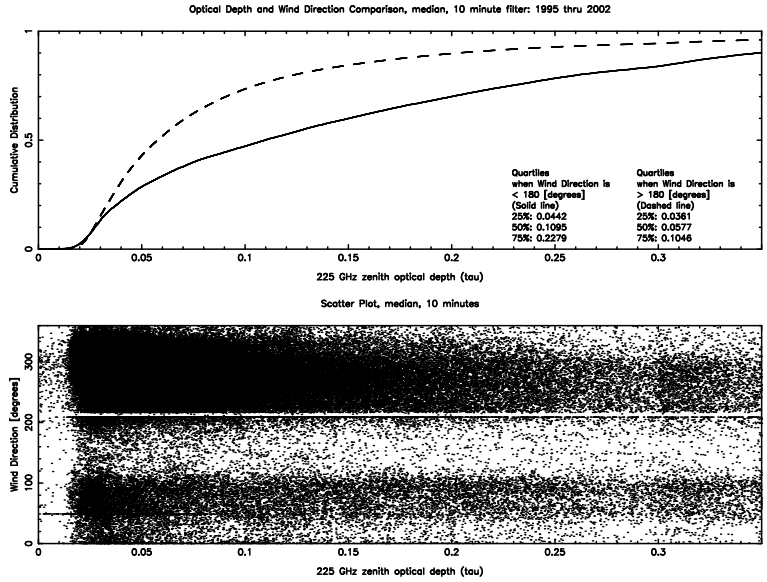

Fig. 8.— Cumulative distributions of the 225 GHz zenith optical depths (τ_{225}) measured at Chajnantor during westerly and easterly winds.

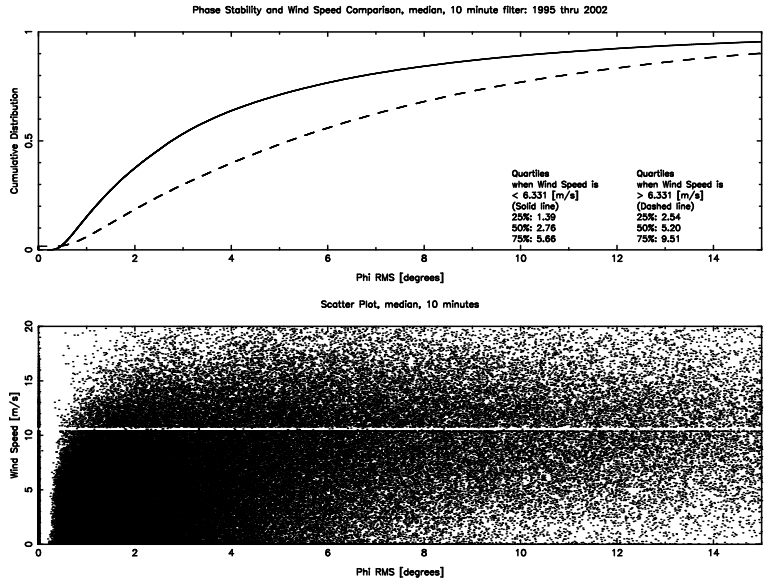

Fig. 9.— Cumulative distributions of the maximum 11.2 GHz phase fluctuations measured at Chajnantor when the wind speed was above or below the median.

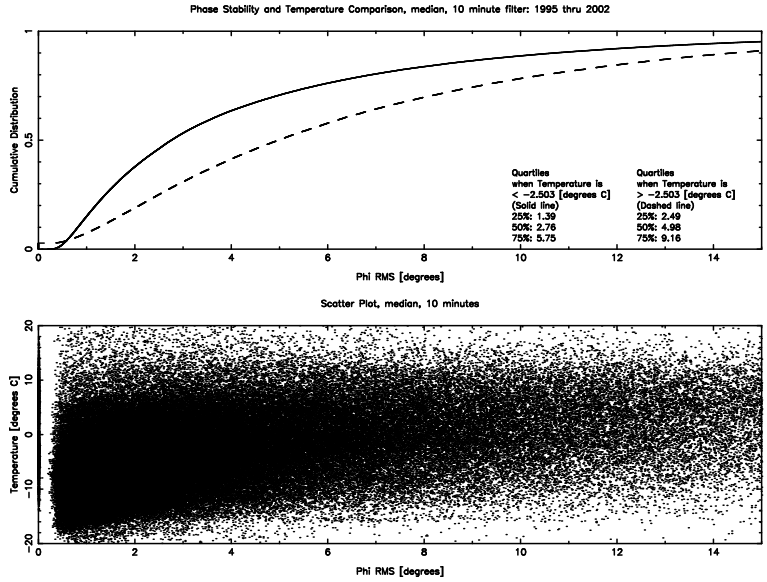

Fig. 10.— Cumulative distributions of the maximum 11.2 GHz phase fluctuations measured at Chajnantor when the temperature was above or below the median.

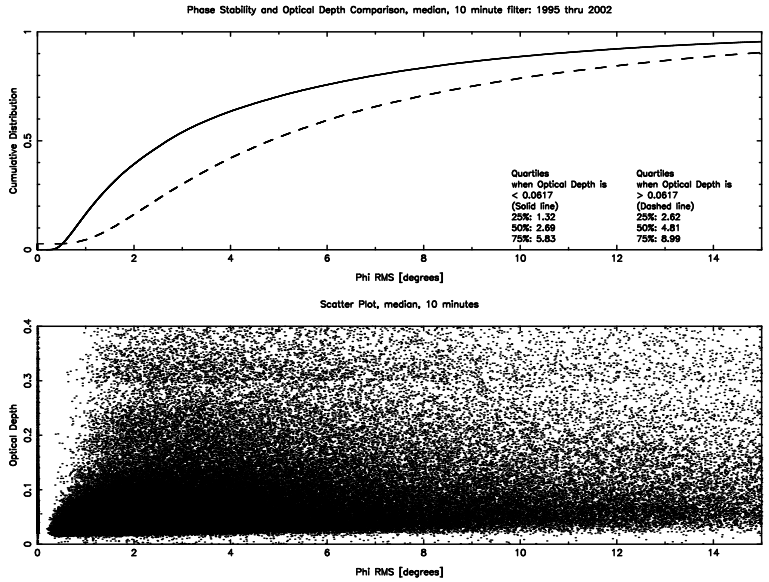

Fig. 11.— Cumulative distributions of the maximum 11.2 GHz phase fluctuations measured at Chajnantor when the 225 GHz zenith optical depth (τ_{225}) was above or below the median.

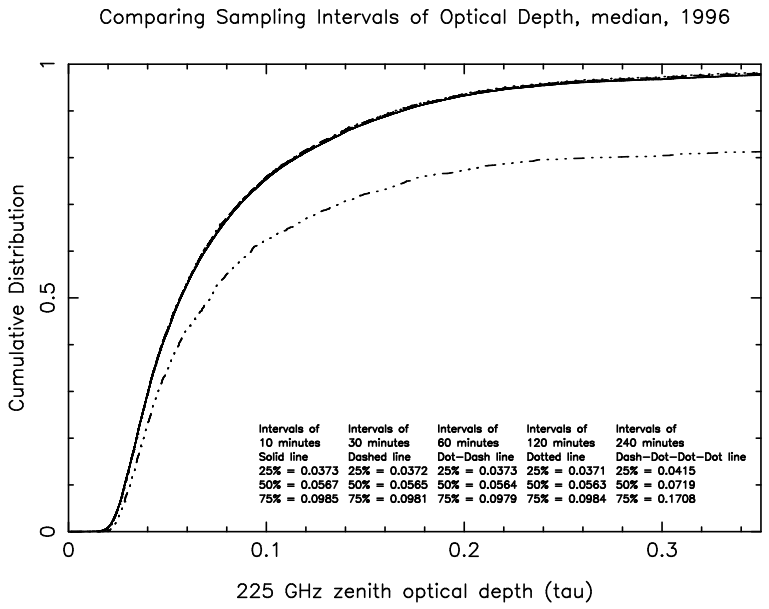

Fig. 12.— Cumulative distributions of the median 225 GHz zenith optical depths (τ_{225}) measured at Chajnantor in 1996 for different sampling intervals. The 240 min interval suffers from a processing defect.